Discontinuous Unbinding Transitions of Filament Bundles

Jan Kierfeld, Torsten Kühne, and Reinhard Lipowsky
Max-Planck-Institut für Kolloid- und Grenzflächenforschung, 14424 Potsdam, Germany
(Received 15 September 2004; published 14 July 2005)

Bundles of semiflexible polymers such as actin filaments are studied theoretically. The bundle formation is governed by attractive filament interactions mediated by cross-linking sticker molecules. Using a combination of analytical arguments and Monte Carlo simulations, it is shown that the formation of bundles of parallel filaments requires a threshold concentration of linkers which becomes independent of the filament number for large bundles. The unbinding of bundles happens in a single, discontinuous transition. We discuss the behavior of the bundle thickness at and below the transition. In the bound phase, large bundles tend to segregate into sub-bundles due to slow kinetics. Our results are in qualitative agreement with experiments on F-actin in the presence of the cross-linking protein α-actinin.

DOI: 10.1103/PhysRevLett.95.038102 PACS numbers: 87.16.Ka, 05.70.Fh, 82.70.−y, 87.16.Ac

Introduction.—Biological cells and chemical synthesis provide a large variety of rodlike filaments. These filaments are semiflexible polymers with a large persistence length L_p and can assemble into different morphologies. Actin filaments, e.g., are characterized by $L_p \simeq 17\ \mu$m [1] and form both bundles [2] and meshworks depending on the presence of different actin-binding linker molecules [2,3]. Since the interfilament attraction is mediated by cross-linkers with weak bonds, the formation of F-actin bundles is reversible and can be controlled by the cross-linker concentration [4–6]. Bundle formation has also been studied in the context of polyelectrolytes, for which charge correlations of polyvalent counterions [7] or counterion aggregation [8] are possible bundling mechanisms. The formation of filament meshworks has been addressed in Ref. [9], focusing on the meshwork topology rather than on the elastic properties of the filaments.

In this Letter, we theoretically study bundle formation and unbinding of N essentially parallel filaments in the presence of cross-linking molecules with two adhesive end groups. It is convenient to confine these filaments within a tubular compartment of length L and diameter $L_\perp$. As shown below, this system exhibits a critical cross-linker concentration, $X_1 = X_{1,c}$, which separates two different concentration regimes. For $X_1 < X_{1,c}$, the filaments are unbound and uniformly distributed within the compartment. For $X_1 > X_{1,c}$, the filaments form either a single bundle, which represents the true ground state of the system as in Figs. 1(a) and 1(c), or several sub-bundles, which represent metastable, kinetically trapped states as in Fig. 1(b). Furthermore, as we decrease the cross-linker concentration from a value above $X_{1,c}$ towards a value below $X_{1,c}$, the bundles undergo a discontinuous unbinding transition at $X_1 = X_{1,c}$.

We explicitly derive this behavior for filaments of fixed length L, but filaments of variable lengths and/or growing filaments should behave in the same way provided the width of the length distribution is small compared to its mean value. Our results are in qualitative agreement with recent experimental observations that bundles of F-actin filaments form above a threshold concentration of cross-linking proteins [4–6]. In these experiments, a stable and narrow length distribution is achieved by adding the protein phalloidin, which inhibits depolymerization, as well as capping proteins such as gelsolin [4–6]. Our theoretical predictions also apply to bundles of microtubules [10] or carbon nanotubes [11].

Model.—In order to model a single bundle we consider N parallel filamentous polymers with bending rigidities κ_i ($i = 1, \ldots, N$), persistence lengths $L_{p,i} = 2\kappa_i/T$ where T is the temperature in energy units, and contour lengths comparable to or smaller than $L_{p,i}$. The filaments are oriented along one axis, say the x axis, and can be parametrized by two-dimensional displacements $\mathbf{z}_i(x)$ perpendicular to the x axis (see Fig. 2) with $0 < x < L$, where L is the projected length of the polymer. Our parametrization is appropriate provided the longitudinal correlation length is small compared to $L_{p,i}$. Since we focus on the unbinding or disassembly process, we can put $L_\perp = \infty$ and, in this way, eliminate one model parameter.

The filament interaction is mediated by cross-linking sticker molecules that adsorb from the surrounding solution. Each linker consists of a short polymer with adhesive end groups; see Fig. 2. In order to describe the linker degrees of freedom, we discretize the filament into seg-

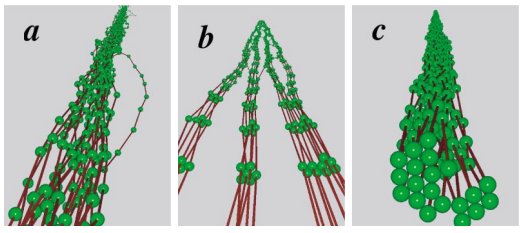

FIG. 1 (color). Monte Carlo snapshots of bundles with $N = 20$ filaments. (a) Close to the unbinding transition in the bundled phase. (b) Deep in the bound phase, the bundle tends to segregate because of slow kinetics and filament entanglement. (c) The equilibrium shape of the bundle is roughly cylindrical.

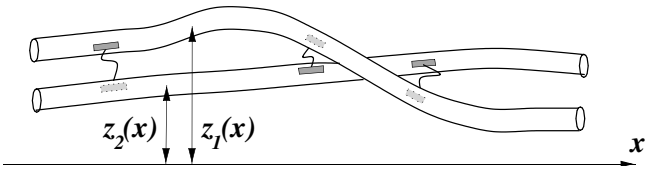

FIG. 2. Cross-linkers connecting two filaments. Each cross-linker consists of two adhesive end groups and a short flexible linker polymer.

ments of length $a_\parallel$, i.e., $x_k = ka_\parallel$ and $\mathbf{z}_{i,k} = \mathbf{z}_i(x_k)$, and introduce occupation numbers $n_{i,k} = n_i(x_k) = 0, 1$ for linkers at segment k of filament i. The segment length $a_\parallel$ is given by the size of the cross-linker end group. The Hamiltonian for the filament-linker system has the form

$$\mathcal{H} = \sum_i [\mathcal{H}_{b,i}\{\mathbf{z}_i\} + \mathcal{H}_1\{n_i\}] + \sum_{i,j} \mathcal{H}_2\{\mathbf{z}_i - \mathbf{z}_j, n_i, n_j\}, \tag{1}$$

where the first contribution $\mathcal{H}_{b,i} = \int_0^L dx \frac{1}{2}\kappa_i(\partial_x^2 \mathbf{z}_i)^2$ contains the bending energies of the filaments with bending rigidities κ_i. The term $\mathcal{H}_1$ describes the intrafilament interactions of linkers. We consider a lattice gas of linkers with hard-core repulsion adsorbing on a filament with $\mathcal{H}_1 = \sum_k a_\parallel W n_{i,k}$ where $W < 0$ is the adhesive energy (per length) of the one linker end group. The third contribution $\mathcal{H}_2$ describes the pairwise interactions between filaments i and j and is given by

$$\mathcal{H}_2 = \sum_k a_\parallel \Big[V_r(\Delta\mathbf{z}_{ij,k}) + \frac{1}{2}(n_{i,k} + n_{j,k} - 2n_{i,k}n_{j,k})V_a(\Delta\mathbf{z}_{ij,k}) \Big], \tag{2}$$

where $\Delta\mathbf{z}_{ij,k} \equiv \mathbf{z}_{i,k} - \mathbf{z}_{j,k}$. The first term is the hard-core repulsion of filaments that is independent of the linker occupation with a potential $V_r(\mathbf{z}) = \infty$ for $|\mathbf{z}| < \ell_r$ and $V_r(\mathbf{z}) = 0$ otherwise where ℓ_r is of the order of the filament diameter. The second term is the linker-mediated attraction and is nonzero if one of the filaments carries a linker. Then the other filament is attracted by a linker-mediated potential $V_a(\mathbf{z})$. The filament can gain an additional energy $|W|$ if it is in a range ℓ_a of the order of the linker size, which we model by a potential well [12]

$$\begin{aligned} V_a(\mathbf{z}) &= W \quad \text{for } 0 < |\mathbf{z}| - \ell_r < \ell_a, \\ V_a(\mathbf{z}) &= 0 \quad \text{otherwise.} \end{aligned} \tag{3}$$

The filament interaction (2) depends only on the coordinate differences $\Delta\mathbf{z}_{ij,k}$. Therefore, the center of mass $\bar{\mathbf{z}}_k \equiv \Sigma_i \mathbf{z}_{i,k}$ of the filament ensemble decouples and performs free diffusion. Bundle formation depends only on $N - 1$ $\bar{\mathbf{z}}_k$-independent displacement fields such as, e.g., $\Delta\mathbf{z}_{1i,k}$ with $i = 2, \ldots, N$.

Now we can trace over the linkers in the grand-canonical ensemble and obtain an effective interaction Hamiltonian $\bar{\mathcal{H}}_2$ [14]. In the limit of low linker densities we find

$$e^{-\bar{\mathcal{H}}_2/T} = \prod_i [(1 - X_1) + X_1 e^{-\Sigma_{j(\neq i)}\Sigma_l a_\parallel (V_r + V_a)/T}] \tag{4}$$

with the linker concentration per site, $X_1 \equiv \langle n_{i,k}, \rangle_1$ where the average is taken with the Hamiltonian $\mathcal{H}_1$. X_1 is determined by the concentration of linkers in solution by $X_1 = Kc_x/(1 + Kc_x)$, where K is the equilibrium constant of the association reaction of the cross-linker with the filament and c_x is the cross-linker concentration in solution. For weakly bound linkers $|W| \ll T/a_\parallel$, we can expand and end up with effective pairwise linker-mediated filament interactions, i.e., $\bar{\mathcal{H}}_2 \approx \Sigma_k a_\parallel [V_r(\Delta\mathbf{z}_{ij,k}) + \bar{V}_a(\Delta\mathbf{z}_{ij,k})]$, which have the same functional form as the bare interactions; the short-range attractive part $\bar{V}_a$ is of the form (3) with a strength $\bar{W} \approx X_1 W$ proportional to the linker concentration on the filament. For strongly bound linkers $|W| \gtrsim T/a_\parallel$, the strength of the short-range attractive part of the effective pair interaction is given by $e^{-a_\parallel \bar{W}/T} = (1 - X_1) + X_1 e^{-a_\parallel \bar{W}/T}$, but higher-order nonpairwise interactions are also generated. Pairwise filament interactions with potentials of the form (3) can also arise from van der Waals, electrostatic, or depletion forces.

Unbinding of two filaments.—The unbinding of two semiflexible polymers with interaction $V_r + \bar{V}_a$ has been studied in detail by transfer matrix methods in Ref. [13]. The unbinding of two filaments was shown to occur at a critical potential strength

$$|\bar{W}_c| \sim (T/L_p)(L_p/\ell_a)^{2/3} \tag{5}$$

(for $\ell_a \gg \ell_r$) where $L_p = 2\kappa_{12}^r/T$ is associated with the reduced bending rigidity $\kappa_{12}^r \equiv \kappa_1\kappa_2/(\kappa_1 + \kappa_2)$ for the relative coordinate $\Delta\mathbf{z}_{12}$. For $|\bar{W}| < |\bar{W}_c|$ filaments are unbound with infinite mean separation $\langle|\Delta\mathbf{z}_{12}|\rangle$, and for $|\bar{W}| > |\bar{W}_c|$ they form a tightly bound state with $\langle|\Delta\mathbf{z}_{12}|\rangle < \ell_a + \ell_r$. The detailed transfer matrix treatment [13] shows that the transition is *discontinuous* in three dimensions. Furthermore, the mean filament separation stays *finite* at the transition, $\langle|\Delta\mathbf{z}_{12}|\rangle \sim \ell_a + \ell_r$, before it jumps to infinity in the unbound phase, whereas the second moment *diverges* as $\langle(|\Delta\mathbf{z}_{12}| - \ell_r)^2\rangle \sim |\bar{W} - \bar{W}_c|^{-1}$ upon approaching the transition. A filament pair thus exhibits pronounced fluctuations close to the unbinding transition even though the transition is first order. These results are confirmed by Monte Carlo (MC) simulations, which also show that the critical exponents do not depend on the presence or absence of the hard-core V_r.

Unbundling of N filaments.—Whereas the critical behavior of two unbinding filaments can be obtained from the exact transfer matrix treatment, this is no longer possible for three or more filaments. Therefore we use an effective 2-polymer model to approach the question whether bun-

dling happens in a single transition. For filaments with very heterogeneous bending rigidities we expect a cascade of two pairwise binding transitions. According to (5), the pair with the highest reduced κ_{ij}^r [say $(ij) = (12)$ assuming that $\kappa_1 \geq \kappa_2 \geq \kappa_3$] binds in a first transition, before the third filament joins the resulting pair bundle in a second transition. Fluctuations of the center of mass of the pair bundle are governed by a rigidity $\kappa_{12}^c \equiv \kappa_1 + \kappa_2$. The binding transition of the third filament is then governed by a reduced rigidity $\kappa_{123} \equiv \kappa_{12}^c \kappa_3/(\kappa_{12}^c + \kappa_3)$ and a potential strength $\bar{W}_{123} = 2\bar{W}$. For both transitions we can calculate the critical potential strength $\bar{W}_c$ using (5). If $|\bar{W}_c|$ is smaller for the second transition, our assumption of a transition cascade is inconsistent. This leads to the criterion $8\kappa_{123} > \kappa_{12}^r$ for the existence of a *single* transition, which is remarkably robust against bending rigidity heterogeneity. For $\kappa_1 = \kappa_2 > \kappa_3$, a single transition exists as long as $\kappa_3 > 0.06\kappa_1$.

For N identical ($\kappa_i = \kappa$) parallel filaments, we proceed similarly and consider the unbinding of two sub-bundles consisting of M and $N - M$ filaments. A sub-bundle of M filaments has a rigidity $\kappa_M^c = M\kappa$, and the unbinding of the two sub-bundles is governed by the reduced rigidity $\kappa_M^r = M(N - M)\kappa/N$. The effective sub-bundle attraction $\bar{W}_M$ is the product of the pair attraction $\bar{W}$ and the difference Δn_{nn} in the number of interacting filament pairs upon separating the sub-bundles, i.e., $\bar{W}_M \sim \bar{W}\Delta n_{nn}$. Applying the result (5) to the two sub-bundles, we find that they unbind at a critical potential strength $\bar{W}_c(M) \sim \bar{W}_c^{\text{pair}} M^{-1/3}/\Delta n_{nn}(M)$ for $N \gg M$, where $\bar{W}_c^{\text{pair}}$ is the critical potential strength for a filament pair. In deriving this result we used that, because of the repulsive part of their interaction, filaments in large bundles interact only with a limited number q of nearest neighbors for short-range attractions as mediated by cross-linkers (this is not the case for sufficiently long-range interactions). We find that $|\bar{W}_c(M)|$ decreases with M such that there is a *single* unbundling transition, which takes place if a single filament losing $\Delta n_{nn} \approx q/2$ nearest neighbors unbinds from the bundle. For large N, this leads to the N-independent result $\bar{W}_c \approx \bar{W}_c(M = 1) \sim 2\bar{W}_c^{\text{pair}}/q$. For small N, $|\bar{W}_c|$ decreases monotonically from the pair value $|\bar{W}_c^{\text{pair}}|$. In the absence of a hard-core repulsion, on the other hand, we expect $|\bar{W}_c|$ to *vanish* as $\sim 1/N$ for large N since all filaments attract each other.

Monte Carlo simulations.—To gain further insight into bundle formation we have performed extensive MC simulations for bundles containing up to $N = 20$ filaments using the effective Hamiltonian $\mathcal{H} = \Sigma_i \mathcal{H}_{b,i} + \Sigma_{i,j} \bar{\mathcal{H}}_2$ which is obtained after integrating out cross-linking stickers. Filaments are discretized into $L/\Delta x$ points along the x direction, in which we apply periodic boundary conditions. In each MC step we attempt a random perpendicular displacement in the z direction. These MC simulations can be used to determine the locus and order of the unbinding transitions since the mean energy $\langle \mathcal{H} \rangle$ (see Fig. 3(a)) exhibits a discontinuity across a first order transition. To gain further insight into bundle morphologies we also measure the mean segment separation $\langle |\Delta \mathbf{z}_{ij}| - \ell_r \rangle$ (see Fig. 3(b)) which is directly proportional to the mean bundle thickness that can be determined by optical microscopy in experiments.

Our MC simulations confirm that for bundles containing up to $N = 20$ filaments there is a single, *discontinuous* unbinding transition; see Fig. 3(a). In the presence of a hard-core repulsion, we also observe saturation of the critical potential strength $\bar{W}_c$ to a N-independent limiting value for large N as predicted analytically. As can be seen in Fig. 1(a), typical bundle morphologies close to the transition are governed by pair contacts of filaments. The bundle thickness, as given by the mean segment separation

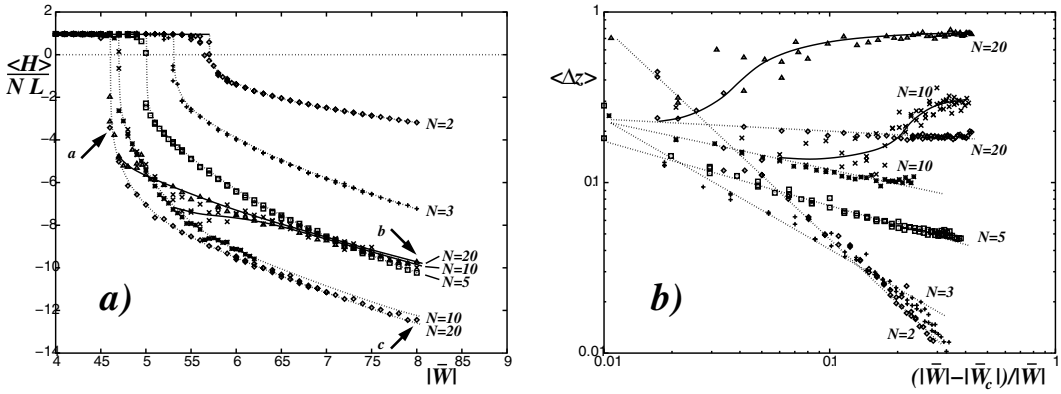

FIG. 3. MC data for $N = 2$, 3, 5, 10, 20 identical filaments (with persistence length $L_p = 200$, contour length $L = 100$, potential range $\ell_a = 0.001$, and hard-core radius $\ell_r = 0.1$; all lengths are in units of Δx; lines are guides to the eye). For $N = 10$, 20 two branches of data are shown corresponding to two different initial conditions; in the lower branch we prepared a compact cylindrical configuration, and in the upper branch (thick lines) we arranged filaments initially in a plane. (a) Mean energy $\langle \mathcal{H} \rangle/NL$ per filament (in units of T) as a function of the effective potential strength $|\bar{W}|$. Arrows correspond to the snapshots in Fig. 1. (b) Logarithmic plot of the mean filament separation $\langle \Delta z \rangle \equiv \langle |\Delta \mathbf{z}_{ij}| - \ell_r \rangle$ (in units of Δx) as a function of the reduced potential strength $(|\bar{W}| - |\bar{W}_c|)/|\bar{W}|$.

$\langle |\Delta \mathbf{z}_{ij}| - \ell_r \rangle$, stays *finite* up to the transition; see MC data in Fig. 3(b). For increasing N, an increasing number of higher moments $\langle (|\Delta \mathbf{z}_{ij}| - \ell_r)^m \rangle$ remains finite at the transition [15] showing that the critical thickness fluctuations of large bundles become small.

Deep in the bundled phase, i.e., for large $|\bar{W}|$, our MC simulations show that bundles do not always reach their equilibrium shape. Small sub-bundles containing typically $N \sim 5$ filaments form easily, they start to entangle, and further equilibration is kinetically arrested suggesting that the bundle is in a ''glass'' phase. Figure 1(b) shows the segregation into sub-bundles in a typical configuration and Fig. 3(a) shows the corresponding rise in the mean bundle energy per filament which approaches the $N = 5$ result. In Fig. 3(b) the pronounced rise of the mean separation for $N > 5$ with increasing potential strength and with increasing N is due to the segregation. This behavior is reminiscent of the experimentally observed F-actin structures consisting of networks of small bundles [5]. Only when starting from a sufficiently compact initial state do bundles relax towards the equilibrium form in the MC simulation, which is a roughly cylindrical bundle with a hexagonal filament arrangement ($q = 6$) as shown in Fig. 1(c). In contrast to the segregated form, the bundle thickness and the mean energy per filament of the equilibrium form decrease with increasing N, as can be seen in Fig. 3. Both types of bundles swell as one increases the hard-core ℓ_r.

Discussion and conclusion.—The critical potential strength $\bar{W}_c$ corresponds to a critical cross-linker concentration $X_{1,c}$. For weakly bound linkers $|W| \ll T/a_\parallel$, we have a simple linear relation $\bar{W} \approx X_1 W$ such that $X_{1,c} \approx \bar{W}_c/W$. The corresponding relation for strongly bound linkers is more complicated. Unbundling can be studied experimentally by (i) isolating a bundle of N filaments from a system at high cross-linker concentration using, e.g., a micropipette, and (ii) transferring the bundle to cross-linker solutions of lower concentration, where it eventually unbinds for $X_1 < X_{1,c}$.

We have shown that long parallel filaments in a finite compartment distribute evenly for $|\bar{W}| < |\bar{W}_c|$, whereas they bind into a single bundle for $|\bar{W}| > |\bar{W}_c|$ [16]. The phase with homogeneously distributed parallel filaments for $|\bar{W}| < |\bar{W}_c|$ can be interpreted as a low-density nematic phase, whereas the bundle that forms for $|\bar{W}| > |\bar{W}_c|$ resembles a domain of a high-density nematic phase which coexists with a phase of small filament density.

In order to include translational and rotational entropy, we can map the ensemble of semiflexible filaments considered here onto an ensemble of rigid rods of length L and diameter $a_\perp$ at a certain concentration c [17]. The effective pairwise attraction (per length) J is given by the bundling free energy of the filaments, which arises from the competition of configurational entropy and short-range attraction and is given by $J \sim \bar{W}_c - \bar{W} > 0$ for $|\bar{W}| > |\bar{W}_c|$ and by $J = 0$ for $|\bar{W}| < |\bar{W}_c|$. As shown in Refs. [17], the hard rod system separates into a high-density nematic phase and a low-density nematic or isotropic phase above a critical attraction, i.e., for $J > J^* = J^*(c, L)$. The critical value J^* behaves as $J^* \sim 1/L$ [17] in the limit of large L, which is consistent with our result that, in the same limit, N parallel filaments form a bundle for $|\bar{W}| > |\bar{W}_c|$ or $J > 0$ corresponding to $J^* = 0$ [16]. The phase separation for $J > J^*$ is in qualitative agreement with the experimental results in Refs. [4–6]. An intermediate gel phase as observed in Ref. [4] is absent in the rigid rod model since this phase is presumably governed by entanglement effects.

In conclusion, we have shown that bundles of long, parallel filaments that adhere via molecular cross-linkers, undergo a single, discontinuous unbinding transition at a finite cross-linker concentration. Therefore, bundle assembly and disassembly can be controlled by varying the cross-linker concentration in the surrounding solution. Large bundles can be kinetically trapped in glasslike states consisting of several sub-bundles.

We thank Marie France Carlier for helpful discussions.

[1] A. Ott *et al.*, Phys. Rev. E **48**, R1642 (1993); F. Gittes *et al.*, J. Cell Biol. **120**, 923 (1993); J. Käs, H. Strey, and E. Sackmann, Nature (London) **368**, 226 (1994).
[2] J. R. Bartles, Curr. Opin. Cell Biol. **12**, 72 (2000).
[3] K. R. Ayscough, Curr. Opin. Cell Biol. **10**, 102 (1998); S. J. Winder, *ibid.* **15**, 14 (2003).
[4] M. Tempel, G. Isenberg, and E. Sackmann, Phys. Rev. E **54**, 1802 (1996).
[5] O. Pelletier *et al.*, Phys. Rev. Lett. **91**, 148102 (2003).
[6] M. L. Gardel *et al.*, Science **304**, 1301 (2004).
[7] B.-Y. Ha and A. J. Liu, Phys. Rev. Lett. **81**, 1011 (1998); B. I. Shklovskii, *ibid.* **82**, 3268 (1999).
[8] I. Borukhov *et al.*, Phys. Rev. Lett. **86**, 2182 (2001).
[9] A. G. Zilman and S. A. Safran, Europhys. Lett. **63**, 139 (2003).
[10] N. Hirokawa, Curr. Opin. Cell Biol. **6**, 74 (1994).
[11] J. Coleman *et al.*, J. Phys. Chem. B **108**, 3446 (2004).
[12] This potential corresponds to the case $\Delta = 0$ in Ref. [13].
[13] J. Kierfeld and R. Lipowsky, Europhys. Lett. **62**, 285 (2003).
[14] R. Lipowsky, Phys. Rev. Lett. **77**, 1652 (1996).
[15] All moments with $m < 2(N-1)(3N-4)/3$ remain finite.
[16] In the parallel filament model, we neglect the translational entropy $S_{\text{tr}} \sim (N-1)\ln(Na_\perp^2/L_\perp^2)$ where $a_\perp$ and $L_\perp$ are the diameter of a single filament and the system's extension perpendicular to the filaments, respectively. This entropic contribution is, indeed, negligible compared to the binding free energy in the limit of large L provided $L_\perp \ll a_\perp N^{1/2} e^{LJq/4T}$.
[17] M. Warner and P. J. Flory, J. Chem. Phys. **73**, 6327 (1980); A. R. Khokhlov and A. N. Semenov, J. Stat. Phys. **38**, 161 (1985).